Scattering and Mode Conversion by a Screen-Like Inhomogeneity Inside a Dielectric Slab Waveguide

Alexander I. Nosich and Andrey S. Andrenko

***Abstract*— In this paper, the interaction of surface guided waves with a perfectly conducting scatterer shaped as a part of circular screen and placed into a dielectric slab waveguide is investigated in mathematically correct manner. Due to the geometry of screen the orginal boundary value problem is reduced to dual series equations treated further by means of the Riemann-Hilbert Problem technique. Based on this approach, the numerical solution can be obtained, theoretically, with any desired accuracy. The reflection, transmission, and radiated-field quantities are computed for both single-mode and multimode slab guides containing cavity-shaped and strip-shaped scatterers.**

I. Introduction

The theory of surface natural modes on regular homogeneous dielectric slab has become a classical part of electromagnetic wave propagation theory [1]. It has numerous applications in microwaves and optics. However, the problems of scattering and conversion of guided modes due to irregularities or scattering objects (Fig. 1) are of much greater interest from both theoretical and practical points of view. As a matter of fact, in most of active and passive microwave integrated circuit devices the principle of operation is based on the modification of a surface mode field by means of discontinuities inside a regular guide. The design and optimization of such devices call for correct treatment of corresponding boundary-value scattering problems.

There is quite a number of inhomogeneities which can be treated accurately. A scatterer of circular cylindrical shape in the travelling surface-wave field was first investigated in [2], [3] which showed the surface wave propagating on deep water to have no reflection from a hard submerged cylinder. The important assumption was the incompressibility of water that led to Laplace equation for the secondary field, thus eliminating any radiation phenomena. Later in [4], [5] the scattering of surface wave on impedance plane from circular and elliptic cylinders by low-frequency asymptotic approach was considered.

A 2-D problem of greater practical interest is the scattering and mode conversion by a circular dielectric cylinder placed inside or outside a dielectric slab. It was investigated first in [6] under approximation of successive reflections from the surfaces of the slab. Correct treatment of this problem was proposed in [7] (for inner scatterer) and independently in [8] (for outer scatterer). Numerical results of the latter investigation were later reported in [9]. This approach is based on the Fredholm 2nd kind integral equation for the electric field inside the object, discretized by expanding in terms of angular functions.

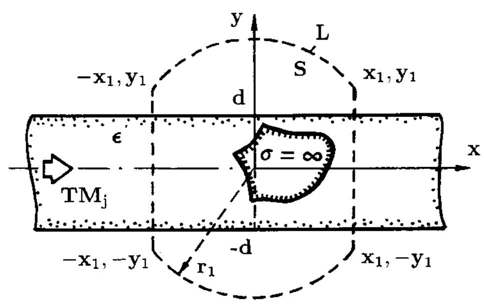

Fig. 1. Perfectly conducting obstacle in a dielectric-slab waveguide.

The 3-D analog of this problem, i.e., spherical scatterer in a circular dielectric waveguide, has been studied approximately in [10], and in correct way in [11]. Later in [12], the boundary integral equation method to study surface deformations was applied, while [13] expanded their approach to longitudinal slab discontinuities. In [14], [15], the principal slab-mode scattering from a single and a pair of perfectly conducting circular cylinders was treated.

As for the scattering of surface wave from a screen-like inhomogeneity, a circular open screen over an impedance plane analytically was studied in [16]. Later, this method was used to study the scattering from screens in a dielectric slab [17], [18]. The aim of this paper is to present an accurate analysis of the scattering and mode conversion of guided modes of slab waveguide by a circular cylindrical open screen placed inside the slab, and to give a review of useful physical information obtained numerically.

The geometry of the problem is shown in Fig. 2. The screen is assumed infinitely thin and perfectly conducting, having the angular width 2δ with an aperture of angular width $2\theta = 2(\pi - \delta)$ positioned at an angle ϕ_0 with respect to the x-axis. The screen is placed at the distance b off the middle of the slab of dielectric constant $\epsilon > 1$ sandwiched between the planes $y = \pm d$ bounding two free lossless halfspaces. Such a slab is known to support finite number of undecaying natural guided modes (surface waves) of two types: TE_j and TM_j. TE/TM notation of modes depends on the field structure

Manuscript received July 2, 1992; revised March 26, 1993. This work was supported in part by Scientific and Technical Research Council of Turkey (TÜBİTAK), in part by Matsumae International Foundation, Japan, under Grant 92007, and in part by Kumamoto University, Kumamoto, Japan..

The authors are with the Institute of Radiophysics and Electronics, Ukrainian Academy of Sciences, 12, Proskura ul., Kharkov, 310085, Ukraine.

IEEE Log Number 9214512.

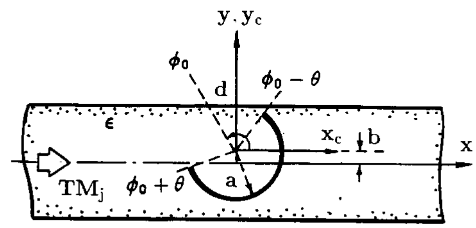

Fig. 2. Open circular screen in a dielectric-slab waveguide. TM_j natural mode is incident.

with respect to the direction of propagation. However, in 2-D scattering problems TE_j modes are obviously E-polarized and TM_j modes are H-polarized with respect to the axis of a scatterer, and this polarization is kept for the scattered field as well.

Our paper is concerned with H-polarization case. Varying the angular width of the screen one can obtain different kinds of obstacles: closed circular bar, slitted circular cavity, circularly curved strip, etc. In Section II, the mathematical formulation of the considered problem is given. Section III presents derivation of energy conservation and reciprocity relationships which couple far-field characteristics of the field. In Section IV, the surface current integro-differential equation is obtained with a kernel determined by the Green's function of the regular slab. Far-field characteristics are constructed in Section V for arbitrary perfectly conducting scatterer. However, the main idea of the treatment is to reduce the initial problem to dual series equations, and to regularize them by the Riemann-Hilbert problem (RHP) technique. This is made in Sections VI and VII, respectively, and results in Fredholm 2nd kind matrix equations solvable numerically with any desired accuracy. Numerical investigation (see Section VIII) was targeted on the reflected and transmitted guided-mode amplitudes for a single-mode guide, as well as mode conversion coefficients for multimode one. Resonant phenomena associated with damped natural oscillations of the screen are analyzed, including low-frequency one due to so-called Helmholtz-mode response. Far-field calculations display the dependence of radiation patterns on the shape of obstacle. We conclude the paper discussing the potential usefulness of screen scatterers for bandstop filtering and antenna applications.

In the following treatment, an $e^{-i\omega t}$ time dependence is assumed for the field and is suppressed throughout the analysis.

II. Formulation of the Problem

Assume a natural guided wave of TM_j type is incident from $x = \mp\infty$ on the inhomogeneous section of waveguide. As electromagnetic field of the mode has no E_z component, it can be determined by means of a single function

$$H^0(\vec{r}) \equiv H^0_{\pm j}(\vec{r}) = V_j(y)e^{\pm ih_j x} \tag{1}$$

corresponding to H_z component. Exact value of the constant of propagation h_j can be found as one of solutions of known characteristic equations (presented in Appendix A) for which $Im h_j = 0$, $k < h_j < k\,\epsilon^{1/2}$, $j = 0, 1, \cdots, Q^{tm}$. Eigenfunctions $V_j(y)$ correspond to the cross-section mode field functions (see Appendix A).

Define the total field through the sum

$$H(\vec{r}) = H^0(\vec{r}) + H^{sc}(\vec{r}). \tag{2}$$

The scattered field $H^{sc}(\vec{r})$ has to satisfy the same homogeneous Helmholtz equation as the incident field $H^0(\vec{r})$

$$[\nabla^2 + k^2\epsilon(y)]H^{sc}(\vec{r}) = 0 \tag{3}$$

where $\epsilon(y) = \epsilon$ for $|y| < d$ or 1 elsewhere, while points $\vec{r} \in \text{ext}(\partial M,\ y = \pm d)$, with ∂M for the cross-sectional contour of the scatterer. It is completed with continuity conditions on the surfaces of the slab (square brackets are for the jumps of functions)

$$[H^0 + H^{sc}] = 0, \qquad y = \pm d \tag{4}$$

$$\left[\frac{1}{\epsilon}\frac{\partial}{\partial y}(H^0 + H^{sc})\right] = 0, \qquad y = \pm d. \tag{5}$$

Besides it must satisfy the Neumann boundary condition at the scatterer

$$\frac{\partial}{\partial n}(H^0 + H^{sc}) = 0, \qquad \vec{r} \in \partial M \tag{6}$$

together with the edge condition which can be formulated as the demand of local energy limitation for any bounded domain $B \in \text{ext}\,\partial M$

$$\int_B (k^2\epsilon|H^{sc}|^2 + |\nabla H^{sc}|^2)\, d\vec{r} < \infty. \tag{7}$$

Finally, to have closed formulation, a condition at infinity is to be imposed. As we assume lossless media ($Im\epsilon = Imk = 0$), we have to take account of the discrete spectrum of slab's natural guided modes $H^0_q(\vec{r})$, $q = 0, 1, \cdots, Q^{tm}$ given by (1). These modes' amplitudes do not decay uniformly for all ϕ as $r \to \infty$ but are constant at $\phi = 0, \pi$. So, the well-known Sommerfeld condition of radiation is obviously not applicable and is to be modified. Thorough analysis of this question (see [19], [20]) yields the following asymptotic requirement at $r \to \infty$

$$H^{sc}(\vec{r}) \sim \begin{Bmatrix} \Phi_j^{(\pm)}(\phi)\left(\frac{2}{i\pi kr}\right)^{1/2}e^{ikr}, & |y| > d \\ 0, & |y| < d \end{Bmatrix} + \sum_{q=0}^{Q^{tm}} \begin{Bmatrix} (T_{qj} - \delta_{qj})H^0_{+q}(\vec{r}), & x > 0 \\ R_{qj}H^0_{-q}(\vec{r}), & x < 0 \end{Bmatrix}. \tag{8}$$

Here $\Phi_j^{(\pm)}(\phi)$ is the far-field scattering pattern associated with jth mode, up and down the slab, δ_{qj} is the Kronecker delta, T_{qj} and R_{qj} are mode conversion coefficients for $q \neq j$ or transmission and reflection coefficients of the incident mode for $q = j$.

To be sure that the function $H(\vec{r})$ solving the boundary-value problem (3) through (8) is unique, one should prove that the difference $\tilde{H}$ between any two solutions is identical zero. Indeed, apply the Green's formula with weight $\epsilon^{-1}(y)$ to function $\tilde{H}$ and its complex conjugate $\tilde{H}^*$ within the domain S bounded by the contour L shown in Fig. 1. Take the limit as $r_1 \to \infty$, $y_1 \to \infty$ but $y_1/r_1 \to 0$ and use the condition of radiation (8) together with orthogonality of modes (1) in the cross-section of slab. Then, we obtain

$$\frac{2}{\pi k d}\int_{-\pi}^{\pi} |\tilde{\Phi}^{(\pm)}(\phi)|^2\, d\phi + \sum_{q=0}^{Q^{tm}} (|\tilde{T}_q|^2 + |\tilde{R}_q|^2) N_q^2 = 0 \quad (9)$$

where N_q is for the norm of the qth mode and is given in Appendix A.

The left-hand part of (9) may be equal to zero if and only if all terms vanish separately. It leads to the conclusion that was sought for.

III. On Energy Conservation and Reciprocity

There are certain general properties of the scattered field valid for arbitrary regular open waveguide containing arbitrary discontinuity of compact nature. We imply the energy conservation and the reciprocity relationships [5], [7], [12], [21], [22]. Their derivation is independent on precise shape of discontinuity. It involves only those of the initial equations that specify field behavior far from irregular section of the guide. Here, we shall follow [20] and use a way which is more formal and also applicable in 3-D case.

Apply Green's formula with weight $\epsilon^{-1}(y)$ to the total field $H(\vec{r}) = H_j^0(\vec{r}) + H^{sc}(\vec{r})$ and its complex conjugate $H^*(\vec{r})$ within the same domain $S \to \infty$ as in Section II. Integration exploits radiation condition and mode orthogonality, and yields

$$N_j^2 = \sum_{q=1}^{Q^{tm}} (|T_{qj}|^2 + |R_{qj}|^2) N_q^2 + P^{(j)} \quad (10)$$

where

$$P^{(j)} = \frac{2}{\pi k d}\int_{-\pi}^{\pi} |\Phi_j^{(\pm)}(\phi)|^2\, d\phi \quad (11)$$

is the power carried to infinity by cylindrical-wave fraction of the total field under the incidence of jth natural mode.

Reciprocity relationship is an expression coupling mode conversion coefficients for two mirror-opposite directions of incidence of the same mode at the same inhomogeneity. In order to obtain it, one has to apply Green's formula with weight once more, now to the pair of functions $H^{(+)} = H_j^0(\vec{r}) + H^{(+)sc}$ and $H^{(-)} = H_{-q}^0(\vec{r}) + H^{(-)sc}$ where $H_{\pm j}^0(\vec{r})$ are given by (1). As both functions satisfy the condition of radiation (8), the final result contains only the field products of incident mode and the surface-mode term of $H^{(\pm)sc}$ of the same index but with opposite sign, namely

$$N_q^2 T_{qj}^{(+)} = N_j^2 T_{jq}^{(-)}. \quad (12)$$

For $j = q$ one obtains simply $T_{jj}^{(+)} = T_{jj}^{(-)}$. It means that transmission of the incident mode is invariant of the direction of incidence.

This property has a well-known counterpart in free-space diffraction. Indeed, forward scattering amplitude of the far-field pattern is the same for two mirror directions of plane wave incidence. For scatterers having a plane of symmetry, like an open circular screen shown in Fig. 2, assume that α is the angle between the plane of symmetry and cross-sectional plane of the waveguide (i.e., for our screen $\alpha = \pi/2 - \phi_0$). Then obviously $T_{qj}^{(\pm)} = T_{qj}(\pm\alpha)$, and from (12) it follows that

$$N_q^2 T_{qj}(\alpha) = N_j^2 T_{jq}(-\alpha) \quad (13)$$

and in particular

$$T_{jj}(\alpha) = T_{jj}(-\alpha). \quad (14)$$

Unlike $T_{jj}^{(\pm)}$, the rest fraction of incident power distributes quite arbitrarily among other modes and cylindrical wave for two different directions of incidence.

A note should be made on the comparison between scattering in open and closed waveguides. One can easily see that in the latter case (10) and (12) are valid as well however the radiation is absent, i.e., $P^{(j)} \equiv 0$. This results in the fact that in closed single-mode guide not only the transmission but also the reflection is the same for two mirror-opposite directions of mode incidence. In an open waveguide this is not true.

Another note concerns application of these relationships for checking the correctness and accuracy of numerical algorithms. They provide convenient and reliable tools of eliminating rough mistakes, however cannot serve as absolute criteria. Both relationships are of far-field nature, so satisfying them is necessary but not sufficient.

IV. Surface Current Equations

In order to proceed to the surface current equation one has to determine the scalar Green's function $G^H(\vec{r}, \vec{r}')$ of the slab. This function can be considered as the field under magnetic-line current source excitation of the slab. It has to satisfy inhomogeneous Helmholtz equation with Dirac-delta in the right-hand part together with conditions (4), (5), and (8). For a slab geometry it has been treated by many authors [1], [7], [12] and can be obtained in terms of Fourier transforms. As our screen is housed inside the slab, we are interested in $G^H(\vec{r}, \vec{r}')$ for a source location at $\vec{r}' = (x', y')$ with $|y'| < d$. Imposing continuity conditions like (4) and (5) on the surfaces $y = \pm d$ and after some straightforward algebra Green's function is found to be

$$G^H(\vec{r}, \vec{r}') = \frac{i}{4}\delta_{l\epsilon} H_0^{(1)}(k\epsilon^{1/2}|\vec{r} - \vec{r}'|) + \frac{i}{4\pi}\int_{C(-\infty,\infty)} F_l(y, y', h) e^{ih(x-x')}\, dh \quad (15)$$

where $l = +, -, \epsilon$, and

$$F_+(y, y', h) = e^{ig(y-d)+ipd} \cdot \left[\left(1 - \frac{g\epsilon}{p}\right)\left(i\frac{B^e(py')B^e(pd)}{\Delta^e(h)} + \frac{B^o(py')B^o(pd)}{\Delta^o(h)}\right) + \frac{1}{p}e^{ipy'}\right]$$

$$F_\epsilon(y, y', h) = e^{ipd}\left(1 - \frac{g\epsilon}{p}\right) \cdot \left[i\frac{B^e(py)B^e(py')}{\Delta^e(h)} + \frac{B^o(py)B^o(py')}{\Delta^o(h)}\right]$$

$$F_-(y, y', h) = e^{-ig(y+d)-ipd} \cdot \left[\left(1 - \frac{g\epsilon}{p}\right) \left(i\frac{B^e(py')B^e(pd)}{\Delta^e(h)} - \frac{B^o(py')B^o(pd)}{\Delta^o(h)} \right) + \frac{1}{p} e^{ipy'} \right] \quad (16)$$

with functions $B^{e,o}(.)$ and $\Delta^{e,o}(.)$ given in Appendix A.

Because of the square-root branching of $g(h)$, Fourier-transform of $G^H(\vec{r}, \vec{r}')$ is the two-valued function of h. It has two branch points at $h = \pm k$ (but not at $h = \pm k\epsilon^{1/2}$ as it can be expanded in terms of power series of p^2).

One can see that the Fourier-transform of $G^H(\vec{r}, \vec{r}')$ is meromorphic function of h varying on the two-sheet Riemann surface of the function $g(h)$. It has complex poles determined by complex zeros of two denominators in (16) which coincide with roots of characteristic equations given in Appendix A. In other words, they correspond to the discrete spectrum of slab's generalized eigen-modes: surface, or proper, modes and leaky modes and other improper modes. For any fixed value of $\kappa = kd(\epsilon - 1)^{1/2}$ there exists finite number $Q^{tm} + 1 \geq 1$ of surface modes and infinite number of leaky-wave modes [1]. As κ is increasing, new leaky-wave poles come in symmetric pairs to the branch points $h = \pm k$ from improper sheet of h-plane and then move as surface-wave poles along the real axis in the proper ("physical") Riemann sheet towards points $h = \pm k\epsilon^{1/2}$.

Consider now the scattering from a perfectly conducting obstacle inside the slab (see Fig. 1). Applying Green's formula with weight to functions $H^{sc}(\vec{r})$ and $G^H(\vec{r}, \vec{r}')$ within the same domain $S \to \infty$ as before and using equation $(\nabla^2 + k^2\epsilon)G^H(\vec{r}, \vec{r}') = -\delta(\vec{r} - \vec{r}')$, one obtains a generalized double-layer potential representation

$$H^{sc}(\vec{r}) = \int_{\partial M} \mu(\vec{r}') \frac{\partial}{\partial n'} G^H(\vec{r}, \vec{r}')\, d\vec{r}'. \quad (17)$$

Here, unknown function $\mu(\vec{r}')$ is the density of surface current induced on the screen and is given by the limit value of the field

$$\mu(\vec{r}) = -H(\vec{r})\,|_{\partial M}\,. \quad (18)$$

To find this function, substituting (17) into (6) yields integro-differential equation

$$\frac{\partial}{\partial n} \int_{\partial M} \mu(\vec{r}') \frac{\partial}{\partial n'} G^H(\vec{r}, \vec{r}')\, d\vec{r}' = -\frac{\partial H^0(\vec{r})}{\partial n}, \quad \vec{r} \in \partial M. \quad (19)$$

The most correct and powerful approach to further treatment of (19) is to regularize it, i.e., to reduce to some matrix operator equation of the Fredholm canonical type

$$(I + T)X = F \quad (20)$$

where I is identity operator and operator T is so-called compact one in some Hilbert space of sequences. This approach gives the way of constructing efficient numerical codes with full mathematical grounding of solution's existence and convergence of computations. As a matter of fact, this procedure is possible in all situations when free-space counterpart of the scattering problem either has analytical solution (as for a circle) or can be regularized itself (as for a flat or circularly curved strip).

V. Evaluation of Far-Field Characteristics

Provided that current density function $\mu(\vec{r})$ has been determined, one can calculate field inside or outside the slab by using (17) at points $\vec{r}$ off the contour ∂M of the obstacle. Let the observation point to be in upper halfspace, i.e., $y > d$. Substituting Fourier-type integral representation (15) for the Green's function into (17) and interchanging the order of integrations lead to the following expression

$$H^{sc}(\vec{r}) = \frac{1}{\pi} \int_{C(-\infty,\infty)} u(h) e^{ig(y-d)} e^{ihx}\, dh, \qquad y > d \quad (21)$$

where

$$u(h) = \frac{i}{4} \int_{\partial M} \mu(\vec{r}') \frac{\partial}{\partial n'} [f_+(y', h) e^{-ihx'}]\, d\vec{r}' \quad (22)$$

and the function $f_\pm(y', h)$ can be obtained from (15) after extracting $e^{ig(\pm y - d)}$.

Thus, calculation of the field as a function of x needs the integration of inverse Fourier-transform like (21). The path of integration C in the physical sheet of Riemann h-plane is shown in Fig. 3 bypassing properly the surface-wave poles at $h = \pm h_q$ on the real axis. If $x \to \pm\infty$, the rapidly oscillating term e^{ihx} enables one to evaluate (21) by using asymptotic technique. The most straightforward approach can be implemented as follows: Assuming $x > 0$ and using the transformation $ih = -s + ik$, one finds that

$$H^s(\vec{r}) = ie^{ikx} \int_{C_1} u(s) e^{ig(y-d)} e^{-sx}\, ds \quad (23)$$

where the contour C_1 running down the imaginary axis in the s-plane as shown in Fig. 4 is the transformed contour C of (21). Deform the branch cut arising from $s = 0$ $(h = k)$ to run to the right along the real s-axis, while the branch cut from $s = 2ik$ $(h = -k)$ to the left. This procedure brings additional (leaky-wave) poles to the s-plane as shown in Fig. 4. Then deform the path C_1 by moving it infinitely far to the right. In accordance with Cauchy theorem the integration yields the sum of residues of all the captured poles plus integral along the branch-cut contour C'. Thus for large positive values of x

$$H^{sc}(\vec{r}) = \sum_{q=0}^{Q^{tm}} (T_{qj} - \delta_{qj}) B_q^{e,o} e^{-\gamma_q(y-d) + ih_q x} + 2\pi i \sum_{m=1}^{\infty} \operatorname{Re} s_{h=h_m} \{u(h)\} e^{ig_m(y-d) + ih_m x} + H_{bc}^{sc}(\vec{r}) \quad (24)$$

where the first (finite) sum is for proper (surface-wave) modes' contribution, while the second (infinite) for leaky-wave modes.

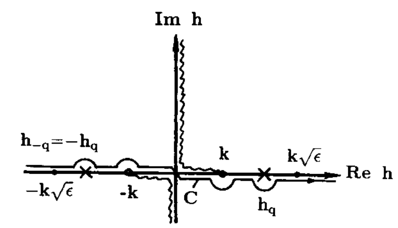

Fig. 3. Complex h-plane and initial integration path C.

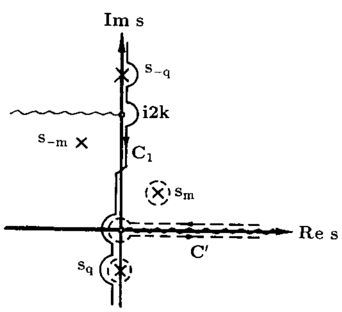

Fig. 4. Complex s-plane and deformed path of integration C'.

The transmitted modes' amplitudes (forward conversion coefficients) are given by

$$T_{qj}-\delta_{qj}=-\frac{1}{2}\operatorname{Re}s_{h=h_q}\int_{\partial M}\mu(\vec{r}')\cdot\frac{\partial}{\partial n'}[f_+(y',h)e^{-ihx'}]\,d\vec{r}'. \quad (25)$$

For large negative values of x similar treatment leads to the result close to (24) but with h_{qj} and $T_{qj}-\delta_{qj}$ replaced by $-h_{qj}$ and R_{qj}, respectively. The following expression for the reflected modes' amplitudes (backward conversion coefficients) is valid

$$R_{qj}=\frac{1}{2}\operatorname{Re}s_{h=h_q}\int_{\partial M}\mu(\vec{r}')\cdot\frac{\partial}{\partial n'}[f_+(y',-h)e^{ihx'}]\,d\vec{r}'. \quad (26)$$

Note, that the second, leaky-wave, term in (24) decays exponentially as $|x|\to\infty$ and may be neglected. The third term (branch-cut integral) is usually referred as lateral wave [1]. It can be shown to vanish algebraically with $|x|\to\infty$ as the main contribution is given by the integration in the vicinity of the branch point $s=0$. In the domain of space defined by conditions $kx\gg k^2(y-d)^2$ and $kx\gg 1$, substituting approximate expression $g^2(s)=s^2-2iks\approx -2iks$ yields $H^s_{bc}(\vec{r})=O(|x|^{-1})$.

Out of the mentioned domain the representation (24) is not reasonable because of the exponential growth of both the second and third terms as $r=[x^2+(y-d)^2]^{1/2}\to\infty$. However the integral (21) can be evaluated by means of the steepest-descent technique [1] assuming that $kr\sin\phi\gg 1$. Introducing new variable of integration $\beta: h=k\cos\beta$, $g=-k\sin\beta$ and following the standard procedure [1], [6], [7], one obtains the cylindrical-wave field (first term in (8)). Far-field patterns are given by

$$\Phi_j^{(\pm)}(\phi)=\sin\phi e^{ikd\sin\phi}\int_{\partial M}\mu(\vec{r}')\cdot\frac{\partial}{\partial n'}[f_\pm(y',k\cos\phi)e^{-ikx'\cos\phi}]\,d\vec{r}' \quad (27)$$

and describe radiation due to the scattering above and below the slab, respectively. Cylindrical wave (27) is usually referred as a space wave in contrast to the surface and leaky waves. As can be easily seen, at infinity, there is no field radiated in grazing directions, i.e., $\phi\to 0,\pi$. Thus along the slab the power is carried entirely by surface guided modes.

In the above derivations, either parameter r or x was assumed large enough to ensure that no real or complex pole effects the expansion of the integrand in terms of power series at the saddle point or the branch point. If this is not true the modified asymptotic-integration technique [1] can be applied.

VI. Dual Series Equations for a Circular Screen

So far we have not exploited the fact that our screen is a part of a circle, as shown in Fig. 2. Let us introduce local coordinates r_c, ϕ_c coaxial with the screen ∂M, such that $x_c=x$, $y_c=y-b$. Then, the surface-current density function $\mu(\vec{r}')\equiv\mu(\phi_c')$, extended by zero to the slot interval $|\phi_c'-\phi_0|<\theta$, can be expanded in terms of angular Fourier series

$$\mu(\phi_c')=\frac{2}{i\pi ka\epsilon^{1/2}}\sum_{n=-\infty}^{\infty}\mu_n e^{in\phi_c'}. \quad (28)$$

The singular part of the Green's function can be expanded as

$$G_0(\vec{r},\vec{r}')\equiv\frac{i}{4}H_0^{(1)}(|\vec{r}-\vec{r}'|)=\frac{i}{4}\sum_{n=-\infty}^{\infty}\begin{Bmatrix}J_n(r')H_n^{(1)}(r), & r>r'\\ H_n^{(1)}(r')J_n(r), & r<r'\end{Bmatrix}e^{in(\phi-\phi')}. \quad (29)$$

In order to expand the regular part of $G^H(\vec{r},\vec{r}')$ we make use of Jakobi-Anger formula

$$e^{ik\cos z}=\sum_{n=-\infty}^{\infty}i^nJ_n(k)e^{inz}. \quad (30)$$

Interchanging the operations of summation and integration and assuming, e.g., that $|y|,|y'|<d$, we find that

$$G^H(\vec{r}_c,\vec{r}_c')-G_0(\vec{r}_c,\vec{r}_c')=\frac{i}{4}\sum_{n=-\infty}^{\infty}J_{-n}(kr_c'\epsilon^{1/2})\sum_{l=-\infty}^{\infty}J_l(kr_c\epsilon^{1/2})\cdot\Omega_{nl}(kb,kd,\epsilon)e^{il\phi_c-in\phi_c'} \quad (31)$$

where we denote

$$\Omega_{nl} = \frac{i^{n+l+1}}{\pi}\int_C e^{ipd}\left(1-\frac{g\epsilon}{p}\right) \cdot \left[i\frac{B^e(n\psi+pb)B^e(l\psi+pb)}{\Delta^e(h)} + \frac{B^o(n\psi+pb)B^o(l\psi+pb)}{\Delta^o(h)}\right] dh \quad (32)$$

and introduce the function $\psi(h)$ through expressions $\cos\psi = h/(k\epsilon^{1/2})$, $\sin\psi = -p/(k\epsilon^{1/2})$.

Substituting series (28), (29), and (31) into (19), exploiting orthogonality of exponents, and taking account of absence of current at the aperture yield the dual series equations

$$\begin{cases} \sum_{n=-\infty}^{\infty}\mu_n\left(J_n' H_n^{(1)'} e^{in\phi_c'} + J_{-n}'\sum_{l=-\infty}^{\infty} J_l'\Omega_{nl}e^{il\phi_c'}\right) \\ \quad = -\sum_{n=-\infty}^{\infty} f_n' e^{in\phi_c'}, \quad \theta < |\phi_c' - \phi_0| \le \pi \\ \sum_{n=-\infty}^{\infty}\mu_n e^{in\phi_c'} = 0, \quad |\phi_c' - \phi_0| < \theta. \end{cases} \quad (33)$$

Here, we imply that arguments of the derivatives of cylindrical functions are $ka\epsilon^{1/2}$. Free-term expansion coefficients are calculated as

$$f_n' = \frac{1}{2\pi}\int_0^{2\pi} \left.\frac{\partial H^0(r_c, \phi_c)}{\partial n}\right|_{r_c=a} e^{-in\phi_c}\, d\phi_c. \quad (34)$$

By using explicit expressions for mode field functions (see Appendix A), we obtain

$$f_n' = i^n J_n' B^{e,o}(n\psi_j - p_j b), \qquad \psi_j = \psi(h_j). \quad (35)$$

The last of initial conditions, that of (7), results in a certain restriction as for coefficients μ_n. Indeed, after integrating the electromagnetic energy over any domain containing the edges, e.g., inside the circle $r_c = a$, one comes to the request that

$$\sum_{n=-\infty}^{\infty} |\mu_n|^2 |n+1| < \infty. \quad (36)$$

VII. Regularization of the Problem

The dual series equations (34) can be rewritten as

$$\begin{cases} \sum_{n=-\infty}^{\infty}\mu_n |n| e^{in\phi} = \Psi(\phi, ka\epsilon^{1/2}), & \phi \in \partial M \\ \sum_{n=-\infty}^{\infty}\mu_n e^{in\phi} = 0, & \phi \in \partial S \end{cases} \quad (37)$$

where ∂M and ∂S are complementary arcs of the same unit circle, and $\Psi(\phi, z)$ is a function, expandable in Fourier series with respect to ϕ. In our particular case,

$$\Psi(\phi, z) = \sum_{n=-\infty}^{\infty}\mu_n \cdot \left[\Delta_n(z)e^{in\phi} - i\pi z^2 J_{-n}'(z)\sum_{l=-\infty}^{\infty} J_l'(z)\Omega_{nl}e^{il\phi}\right] - i\pi z^2 \sum_{n=-\infty}^{\infty} f_n' e^{in\phi} \quad (38)$$

where

$$\Delta_n(z) = |n| + i\pi z^2 J_n'(z) H_n^{(1)'}(z). \quad (39)$$

Equations of this type are often encountered in diffraction theory. In principle, one can directly apply the Method of Moments to solve them numerically. However, there is much more efficient scheme based on inversion of equivalent Riemann-Hilbert Problem (RHP) known in the theory of complex variable [23], [24]. The main factor that makes it possible is that the equivalent RHP is stated here on a unit circle. The dual series operator of (37) is obviously independent of frequency. As $\Psi(\phi, ka\epsilon^{1/2})$ can be shown to vanish at $k \to 0$, we can state that by inverting (37) one inverts the static part of full operator of (33). Omitting the details of this procedure (see [23], [24]), we give the final result in terms of regularized matrix equation

$$[I - A^{(1)} - A^{(2)}]\mu = B \quad (40)$$

where elements of operators $A^{(1)}$, $A^{(2)}$ and vector B are, respectively,

$$A_{mn}^{(1)} = \Delta_n(ka\epsilon^{1/2})S_{mn}(\theta, \phi_0) \quad (41)$$

$$A_{mn}^{(2)} = i\pi k^2 a^2 \epsilon J_{-n}' \sum_{l=-\infty}^{\infty} J_l' \Omega_{nl}(kb, kd, \epsilon) S_{ml}(\theta, \phi_0) \quad (42)$$

$$B_m = i\pi k^2 a^2 \epsilon \sum_{n=-\infty}^{\infty} f_n' S_{mn}(\theta, \phi_0) \quad (43)$$

with functions $S_{mn}(\theta, \phi_0)$ given in Appendix B.

Operator $A^{(1)}$ is compact in the space l^2, i.e., double series of squared matrix elements converges in absolute sense. Operator $A^{(2)}$ is of the same type provided that the screen ∂M does not intersect the interfaces of the slab at $y = \pm d$. Besides, for any parameters of the screen and the slab, vector $B \in l^2$. Furthermore, the full equivalence can be established between the regularized operator equation (40) and initial boundary-value problem of Section II [23]. Hence the solution of (40) is ensured to be unique at least for real k. Based on Fredholm theorems, this is enough to state that it does exist in l^2 and, moreover, satisfies (36). Besides, Fredholm's character of (40) guarantees that theoretically we can approach the exact solution with any desired accuracy by solving truncated matrix of appropriate size. The convergence here is uniform pointwise one, which is not a common place for equations obtained by the Method of Moments.

Expressing far-field values in terms of the surface-current coefficients μ_n, we obtain after some manipulations, that

$$\begin{pmatrix} T_{qj} - \delta_{qj} \\ R_{qj} \end{pmatrix} = -\frac{2e^{ip_q d}}{D_q}\left(1 - \frac{g_q\epsilon}{p_q}\right) \cdot \sum_{n=-\infty}^{\infty} \mu_n (\mp i)^n J_n' B^{e,o}(p_q b \pm n\psi_q) \quad (44)$$

$$\Phi_j^{(\pm)}(\phi) = \frac{k\sin\phi e^{ip'd}}{p'} \sum_{n=-\infty}^{\infty} \mu_n (-i)^n J_n' \cdot \left[(\epsilon' g - p')\left(\frac{B^e(p'd)B^e(n\psi' + p'b)}{i\Delta^e(h')} \mp \frac{B^o(p'd)B^o(n\psi' + p'b)}{\Delta^o(h')}\right) + e^{\mp ip'b \mp in\psi'}\right]. \quad (45)$$

Here, we use functions $D_q = \partial\Delta^{e,o}/\partial h \, |_{h=h_q}$ given at Appendix A, and denote the functions taken at $h = k\cos\phi$ through primed values.

VIII. Numerical Results and Discussion

Computations for both single-mode and multimode inhomogeneous slab guides have been made employing numerical procedure to the equations obtained in previous sections. A simple empiric rule has been verified: to have 0.1 percent accuracy of computing T^{qj}, R^{qj}, the order of truncation of (40) can be taken as integer part of $ka\epsilon^{1/2}$ plus 5.

Before reviewing the results of computations it is worth to note that field behavior has certain common features with free-space scattering from similar open screen. In preceding works (see [23], [24] and the references in these papers) it has been shown that a screen having narrow slot behaves like a cavity-backed aperture. It gives a resonant response provided that the incident wave frequency comes close to the real part of one of the screen's complex natural frequencies. The latters correspond to two families of modes denoted as H^{+}_{mn} $(m \geq 0)$ and H^{-}_{mn} $(m \geq 1)$ because of the splitting of doubly-degenerated modes of closed circular cylinder by cutting a slot. The narrower the slot, the sharper the resonant peaks of total scattering cross-section [23]. Excitation of resonant field inside cavity is equivalent to the appearance of intensive secondary magnetic-line source (or pair of such sources) at the place of slot. As a result, far-field resonant pattern is dominated by the radiation of this secondary source, while far from resonant frequency it is similar to that of closed cylinder. One can observe that H^{-}_{mn} resonances have larger Q-factor than H^{+}_{mn} ones. Besides there exists a specific low-frequency resonance (first reported in [25]) associated with so-called Helmholtz mode and denoted as H^{+}_{00}. Its characteristic frequency is a complex number tending to zero together with θ as $a^{-1}[-2\ln\sin(\theta/2)]^{-1/2}$. This resonance is remarkable for destroying totally the Rayleigh law for H-scattering from small cylinders. When the aperture is widened, resonant phenomena shift to higher frequencies and damp in amplitude however remain observable.

As for the dielectric-slab mode scattering, in practice it is often desired to have a single-mode operation. To support a single (even) TM_0 mode propagation, one has to take the slab characterized with parameter $\kappa = kd(\epsilon - 1)^{1/2} < \pi/2$. This guided mode is called a principal one as it has no low-frequency cutoff unlike the higher-order modes. If $\kappa > \pi/2$, the first higher-order mode, namely odd TM_1, can propagate, and so on.

Fig. 5 shows dependences of amplitudes and phases of reflection and transmission coefficients on relative radius a/d of the screen inside a single-mode slab with κ =1.118. Maximum values are obtained at resonance due to excitation of Helmholtz (H^{+}_{00}) mode of slitted cavity. In this case transmission is very low, the power being partly reflected and partly scattered off the slab. Thus, such an inhomogeneity serves as a resonant bandstop filter, the level of rejection being the function of aperture location and width.

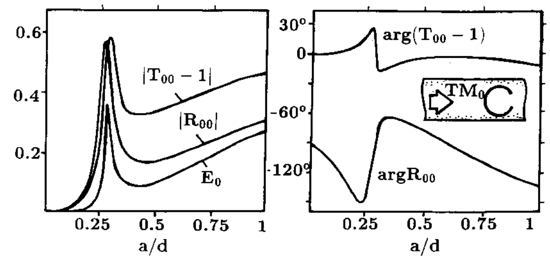

Fig. 5. Amplitudes and phases of principal mode TM_0 versus a/d, for a single-mode slab with kd = 1, ϵ =2.25 housing cavity-shaped screen with θ = 10°, ϕ_0 = 0, b = 0.

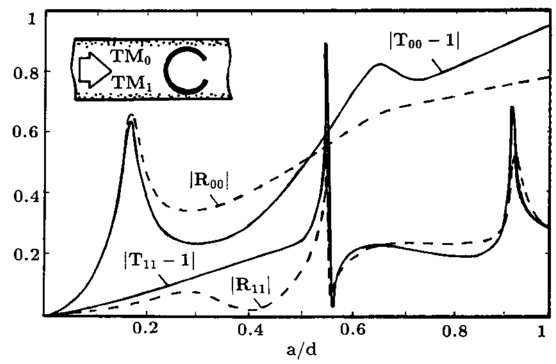

Fig. 6. Amplitudes of reflection and transmission coefficients versus a/d for a cavity-shaped screen with $\theta = 30°$, $\phi_0 = 0$, $b = 0$ inside a two-mode slab with kd =2.3, ϵ =2.25. First-even TM_0 and first-odd TM_1 modes are incident.

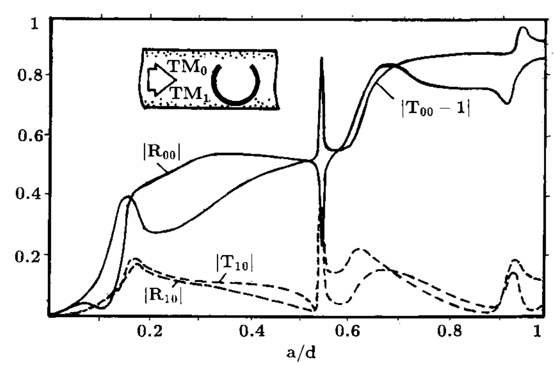

Fig. 7. Amplitudes of mode conversion coefficients versus a/d for the same geometry as in Fig. 6 but with screen rotated at ϕ_0 = 90°. First-even mode TM_0 is incident.

Analogous dependences plotted in Figs. 6 and 7 have been computed for the two-mode slab with κ =2.471. Either TM_0 or TM_1 mode is assumed incident on the screen placed at the center of the slab (b = 0). In general, one can see that the effect of inhomogeneity is greater on even TM_0 mode than on odd TM_1 one due to concentration of guided-mode field in the central part of the slab. If the screen is

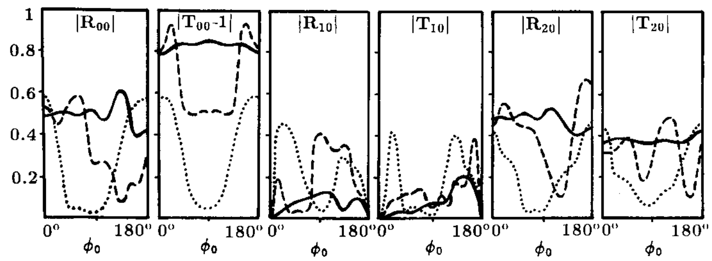

Fig. 8. Effect of screen rotation on the amplitudes of mode conversion coefficients. Screens' parameters are a/d =0.66, b = 0,———— θ = 30°, — — — —θ = 90°,· · · θ = 150° (δ = 30°). Slab parameters are kd =5, ϵ =2.25.

positioned symmetrically with respect to the slab's interfaces, like in Fig. 6, then even/odd guided modes excite separate families of screen's resonances. They are H^+_{00}, H^+_{11}, $H^+_{21}\cdots$, or H^-_{11}, $H^-_{21}\cdots$, depending on the even/odd nature of the incident mode. For arbitrary orientation of aperture (see Fig. 7) any guided mode excites resonances of both types. Note that resonant phenomena associated with H^-_{11} oscillation can result in efficient conversion of TM_0 mode into TM_1 one. This happens because the slot at resonance radiates as intensive secondary line source displaced off the center of the slab.

If a screen is shaped as a curved strip rather than a cavity (i.e., $\delta < \theta$), the resonances are obviously weaker. Intensities of scattering and mode conversion depend mainly on the orientation of the strip, being minimum at grazing incidence.

The plots in Fig. 8 demonstrate the effect of screen rotation on mode conversion coefficients for a four-mode slab (κ =5.56) under TM_0 mode incidence. The curves for three screens of the same radius but of different widths are presented. Here, the screen having aperture of $\theta = 30°$ produces resonant response corresponding to Helmholtz-mode (H^+_{00}). One can easily see that $T_{00}(\pi/2 + \phi_0) = T_{00}(\pi/2 - \phi_0)$ exactly as it is demanded by reciprocity relationship (14). Actual agreement is not worse than up to seven digits that serves as partial proof of algorithm's accuracy. Besides, one can see that effect of a narrow slot is more pronounced when it is seen by incident wave, and weaker when it is in shadow region. Cylindrical strip disturbs incident mode in slightest manner provided that it is positioned at $\phi_0 = \pi/2$ where all the curves have deep minima.

Open waveguides obviously differ from closed ones by the presence of radiation off the guide due to inhomogeneity. Directivity properties of this radiation are described by far-field scattering patterns $\Phi(\phi)$. Fig. 9 shows field patterns of cylindrical wave radiated at H^+_{00} resonance excited by a TM_0 mode of a single-mode slab. Similarly to the scattering from dielectric obstacle [6], [12], effect of the slab can be observed in suppressing the radiation in forward and backward grazing directions. As free-space scattering at the same resonance produces almost omnidirectional patterns [23], [25], main lobes radiate broadside up and down the slab. Note that far-zone amplitudes of the field scattered from closed cylinder of the same radius are much smaller. For two-mode slab, as in Fig. 10, far-field patterns exhibit several lobes of radiation both above and below the guide.

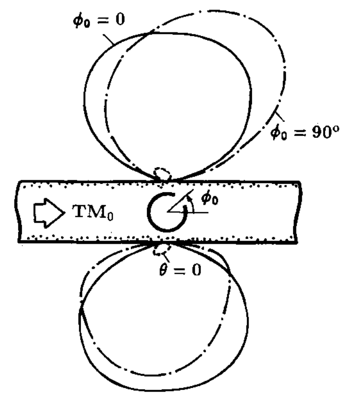

Fig. 9. Far-field power patterns due to the scattering of TM_0 mode from a cavity-shaped screen having θ = 30°, a/d =0.25, b = 0, at two different positions of the aperture. Slab parameters are kd = 1, ϵ =2.25. Dashed line is for a circular bar of the same radius.

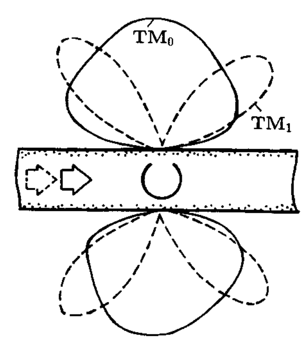

Fig. 10. Far-field power patterns due to the scattering of TM_0 and TM_1 (dashed line) modes from a cavity-shaped screen with θ = 30°, ϕ_0 = 90°, a/d = 0.53, b = 0 inside a two-mode slab with kd =2.3, ϵ =2.25.

Interesting result is obtained for the scattering by a cylindrical strip (Fig. 11). If the strip is placed in the center of the slab and TM_0 mode is incident, the radiation can be highly directional. Similar effect is observed for a strip displaced off the center of the slab if the odd TM_1 mode is incident. Main beam direction correlates with strip's angular position, and sidelobe level is relatively low.

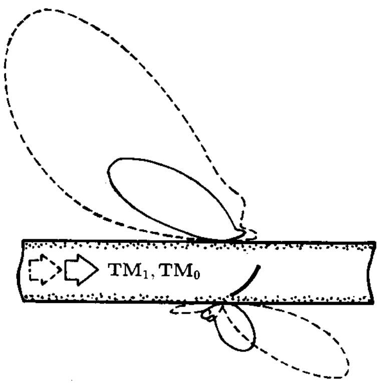

Fig. 11. Same as Fig. 10 but for a circular strip with $\delta = 52°$, $\phi_0 = 142°$, $a/d = 1.29$, $b/d = 0.345$ inside a slab with $kd = 5.8$, $\epsilon = 2.25$.

Note, the absence of multiple deep ripples in patterns of Figs. 9–11 characteristic for similar patterns in [6], [12]. This may be explained by much greater slab thickness in the latter case, and agrees with results presented in [14], [15].

IX. Conclusions

In this paper, we have considered the effect of an open cylindrical-screen inhomogeneity on guided-mode propagation in dielectric slab. The approach used here is based on analytical inversion of a part of initial operator. Results are given in terms of Fredholm 2nd kind algebraic equations, and the rapid convergence of numerical algorithm to exact solution is guaranteed. Numerical data are presented for TM_0 and TM_1 mode scattering in single-mode and multimode slabs.

Sharp resonant phenomena are observed for the scattering by cavity-shaped screens due to internal resonances. The latter have damped behavior because of the coupling both to radiation field and guided modes fields. Most interesting is the Helmholtz-type resonance destroying Rayleigh's law of scattering by small objects. This effect can be exploited for designing miniature bandstop filters in dielectric waveguides and integrated circuits. As for a cylindrical strip placed into the slab, it is shown to produce directive radiation patterns even if being not wider than several wavelengths. So, the strip exhibits all the features of a quasi-optical mirror and can be useful for antenna applications.

A final remark should be made that analogous treatment can be developed for alternative polarization involving E-type Green's function and partial inversion procedure.

X. Appendix A

Characteristic equations for even and odd modes TM_j on a uniform dielectric slab are respectively,

$$\Delta^e(h) \equiv ig\epsilon B^e(pd) + pB^o(pd) = 0 \qquad (46)$$

$$\Delta^o(h) \equiv ig\epsilon B^o(pd) - pB^e(pd) = 0 \qquad (47)$$

where $g^2 = k^2 - h^2$, $p^2 = k^2\epsilon - h^2$, $B^e(x) = \cos x$, $B^o(x) = \sin x$, $B_j^{e,o} = B^{e,o}(p_j d)$.

Provided that $Imk = Im\epsilon = 0$, these two equations have in all $Q^{tm} + 1 \geq 1$ purely real roots h_j, $j = 0, 1, \cdots, Q^{tm}$ representing wavenumbers of natural guided TM_j modes (eigenmodes), with $j = 2n$ for even modes and $j = 2n + 1$ for odd modes ($n = 0, 1, \cdots$). Corresponding eigenfunctions are obtained as

$$V_j(y) = \begin{cases} B^{e,o}(p_j y), & |y| \leq d, \\ B_j^{e,o} \exp[-\gamma_j(|y| - d)], & |y| \geq d \end{cases} \qquad (48)$$

where we denote $\gamma_j = (h_j^2 - k^2)^{1/2}$.

Guided-modes' fields are known to satisfy orthogonality expressions like

$$\int_{-\infty}^{\infty} \frac{1}{i\epsilon} H_j^0 \frac{\partial}{\partial x} H_g^{0*}\, dy = h_q \int_{-\infty}^{\infty} \frac{1}{\epsilon} V_j V_q\, dy = kdN_j^2 \delta_{jq} \qquad (49)$$

with norm of the mode given by

$$N_j^2 = \frac{h_j}{k}\left[\frac{1}{\epsilon} + (-1)^j \frac{\sin 2p_j d}{2\epsilon p_j d} + \frac{(B_j e,\, o)^2}{\gamma_j d}\right]. \qquad (50)$$

Coefficients D_j introduced in (44) are calculated to be

$$D_j = h_j\left[B_j^{o,e} \frac{i\epsilon g_j d - 1}{p_j} \mp B_j^{e,o} \frac{i\epsilon + g_j d}{g_j}\right]. \qquad (51)$$

XI. Appendix B

Calculation of coefficients $S_{mn}(\theta, \phi_0)$ yields [23], [24]

$$S_{mn}(\theta, \phi_0) = (-1)^{n+m} e^{i(n-m)\phi_0} \cdot \begin{cases} W_{mn}(-\cos\theta), & m \neq 0 \\ W_{n0}(-\cos\theta), & m = 0,\ n \neq 0 \\ -\ln[(1 - \cos\theta)/2], & m = n = 0 \end{cases} \qquad (52)$$

where the functions of angular width of the aperture are combined of the Legendre polynomials P_n of the same argument

$$W_{mn} = \frac{P_{m-1}P_n - P_m P_{n-1}}{2(m - n)}, \qquad m \neq n \qquad (53)$$

$$W_{mm} = \frac{\text{sign}\,(m)}{2m} \sum_{s=0}^{|m|} q_{|m|-s} P_{|m|-s-1} \qquad (54)$$

where $q_0(x) = 1$, $q_1(x) = -x$, $q_{s>1}(x) = P_s(x) - 2xP_{s-1}(x) + P_{s-2}(x)$.

References

[1] L. B. Felsen and N. Marcuvitz, *Radiation and Scattering of Waves*. Englewood Cliffs, NJ: Prentice-Hall, 1973.

[2] W. R. Dean, "On the reflection of the surface waves by a submerged circular cylinder," *Proc. Cambridge Phyl. Soc.*, vol. 44, pp. 483–491, 1948.

[3] F. Ursell, "Surface waves on deep water in the presence of a submerged circular cylinder," *Proc. Cambridge Phyl. Soc.*, vol. 46, pp. 141–158, 1950.

[4] A. L. Cullen, "Reflection from cylinder in surface-wave field," *Electron. Lett.*, vol. 11, pp. 479–480, 1975.

[5] M. J. Davis and F. G. Leppington, "The scattering of electromagnetic surface waves by circular and elliptic cylinders," *Proc. Roy. Soc. London*, vol. 533-A, pp. 55–75, 1977.

[6] N. Morita, "Scattering and mode conversion of guided modes of a slab waveguide by a circular cylinder," *Proc. IEE*, vol. 127, part H, pp. 263–269, 1980.
[7] N. K. Uzunoglu and J. G. Fikioris, "Scattering from an inhomogeneity inside a dielectric-slab waveguide," *J. Optical Soc. Am.*, vol. 72, pp. 628–637, 1982.
[8] V. I. Kalinichev and V. F. Vzyatishev, "Natural and forced oscillations in open resonant structures based on disk dielectric resonators," *Izvestiya Vuzov Radiofizika*, vol. 26, pp. 475–482, 1983 (English Transl. *Radiophys. Quant. Electron.*, vol. 26, 1983).
[9] V. I. Kalinichev and P. N. Vadov, "Numerical investigation of disk dielectric resonator excited by Dielectric Waveguide," *Radiotekhnika i Elektronika*, vol. 33, pp. 464–473, 1988 (English Transl. *Sov. J. Commun. Technol. Electron.*, vol. 33, 1988).
[10] N. Morita and N. Kumagai, "Scattering and mode conversion of guided modes by a spherical object in an optical fiber," *IEEE Trans. Microwave Theory Tech.*, vol. MTT-28, pp. 137–141, 1980.
[11] N. K. Uzunoglu, "Scattering from inhomogeneities inside a fiber waveguide," *J. Optical Soc. Am.*, vol. 71, pp. 259–273, 1981.
[12] N. Morita, "An integral equation method for electromagnetic scattering of guided modes by boundary deformations of dielectric slab waveguides," *Radio Sci.*, vol. 18, pp. 39–47, 1983.
[13] P. G. Cottis and N. K. Uzunoglu, "Analysis of longitudinal discontinuities in dielectric slab waveguides," *J. Optical Soc. Am.*, vol. A-1, pp. 206–215, 1984.
[14] V. I. Kalinichev and N. M. Soloviov, "Diffraction of surface waves from two metal cylinders," *Radiotekhnika i Elektronika*, vol. 34, pp. 2245–2250, 1989 (English Transl. *Sov. J. Commun. Techn. Electron.*, vol. 35, 1990).
[15] V. I. Kalinichev, "Scattering of surface waves from a metal cylinder in a dielectric waveguide," *Radiotekhnika i Elektronika*, vol. 36, pp. 259–266, 1991 (English Transl. *Sov J. Commun. Techn. Electron.*, vol. 36, 1991).
[16] A. I. Nosich, "Scattering of the surface wave of an open impedance waveguide by an unclosed cylindrical screen," *Sov. Phys.-Techn. Phys.*, vol. 31, pp. 883–889, 1986.
[17] A. S. Andrenko, A. I. Nosich, and V. P. Shestopalov, "Reciprocity theorem in problems concerning the scattering of waves by irregularities in open planar waveguides," *Sov. Phys. Doklady*, vol. 35, pp. 366–368, 1990.
[18] A. S. Andrenko and A. I. Nosich, "H-scattering of thin-film modes from periodic gratings of finite extent," *Microwave Optic. Technol. Lett.*, vol. 5, pp. 333–337, 1992.
[19] A. I. Nosich, "Radiation conditions for open waveguides," *Sov. Phys. Doklady*, vol. 32, pp. 720–722, 1987.
[20] ——, "On correct formulation and general properties of wave scattering by discontinuities in open waveguides," *Proc. Int. Seminar Math. Methods Electromagn. Theory*, Gurzuf, Ukraine, 1990, pp. 100–112.
[21] P. G. Petropoulos and G. A. Kriegsmann, "Optical theorems for electromagnetic scattering by inhomogeneities in layered dielectric media," *IEEE Trans. Antennas Propagat.*, vol. 39, pp. 1119–1124, 1991.
[22] K. Tanaka and M. Kojima, "Volume integral equations for analysis of dielectric branching waveguides," *IEEE Trans. Microwave Theory Tech.*, vol. MTT-36, pp. 1239–1245, 1988.
[23] A. I. Nosich, "Green's function—Dual series approach in wave scattering by combined resonant scatterers," in M. Hashimoto, M. Idemen and O. A. Tretyakov (Eds.), *Analytical and Numerical Methods in Electromagnetic Wave Theory.* Tokyo: Science House, 1993, pp. 449–469.
[24] R. W. Ziolkowski, "n-series problems and the coupling of electromagnetic waves to apertures: A Riemann-Hilbert approach," *SIAM J. Math. Anal.*, vol. 16, pp. 358–378, 1985.
[25] A. I. Nosich and V. P. Shestopalov, "An electromagnetic analog of a Helmholtz resonator," *Sov. Phys. Doklady*, vol. 22, pp. 251–253, 1977.

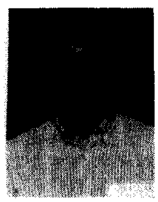

Alexander I. Nosich was born in Kharkov, Ukraine in 1953. He obtained the M.S., Ph.D., and Doctor of Sciences degrees in Radio Physics from Kharkov University, Kharkov, Ukraine, in 1975, 1979, and 1990, respectively.

Since 1979, he has been with the Institute of Radiophysics and Electronics of the Ukrainian Academy of Sciences, Kharkov, as a Junior and Senior Scientist. From February to August 1992, he was with Bilkent University, Ankara, Turkey as a Visiting Professor. From September 1992 to March 1993, he was with Kumamoto University, Japan, as Research Fellow of the Matsumae Foundation, where he is currently a Visiting Associate Professor. His research interests are in antenna simulation, diffraction from screens and gratings, electromagnetic propagation, and scattering in open waveguides.

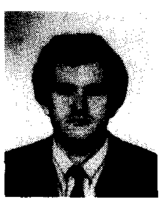

Andrey S. Andrenko was born in Kharkov, Ukraine, in 1964. He received the M.S. and Ph.D. degrees in Radiophysics from Kharkov State University, Kharkov, Ukraine, in 1986 and 1992, respectively.

Since 1991, he has been a Research Scientist in the Electronics Department of the Institute of Radiophysics and Electronics Ukrainian Academy of Sciences, Kharkov, Ukraine. Currently, he is a Visiting Assistant Professor at Gaziantep University, Turkey. His research interests include microwave field theory, theory of diffraction and wave transformation in open waveguides with inhomogeneities.